Am J Transl Res 2016;8(11):4922-4931
www.ajtr.org /ISSN:1943-8141/AJTR0037674

Original Article

Magnetic resonance elastography in a rabbit model of liver fibrosis: a 3-T longitudinal validation for clinical translation

Liqiu Zou[1], Jinzhao Jiang[2], Wenxin Zhong[1], Chunrong Wang[1], Wei Xing[3], Zhuoli Zhang[4,5]

[1]Department of Radiology, Shenzhen Nanshan District People's Hospital, Shenzhen, China; [2]Department of Radiology, Hong Kong University Shenzhen Hospital, Shenzhen, Guangdong, China; [3]Department of Radiology, Affiliated Third Hospital of Suzhou University, Changzhou, Jiangsu, China; [4]Department of Radiology, Northwestern University Feinberg School of Medicine, Chicago, IL, USA; [5]Robert H. Lurie Comprehensive Cancer Center, Chicago, IL, USA

Received August 10, 2016; Accepted November 2, 2016; Epub November 15, 2016; Published November 30, 2016

Abstract: This study aimed to determine the relationships between magnetic resonance elastography (MRE) imaging biomarkers and the stages of liver fibrosis in a rabbit model of liver fibrosis, a longitudinal validation for clinical translation. Liver fibrosis was induced in 38 male New Zealand rabbits by weekly subcutaneous injections of 0.1 ml 50% carbon tetrachloride oily solution per kilogram of body weight for 4 to 10 weeks to produced varying degrees of liver fibrosis. The values for the liver stiffness (LS) MRE imaging biomarkers were measured at different stages of liver fibrosis. Masson trichrome staining of liver tissue was used to identify collagen tissue. Among the 38 rabbits, the histological studies showed liver fibrosis stage 1 (F1, n = 11), liver fibrosis stage 2 (F2, n = 8), liver fibrosis stage 3 (F3, n = 7), and liver fibrosis stage 4 (F4, liver cirrhosis, n = 12). Additional healthy rabbits served as controls (F0, n = 15). During liver fibrosis progression, the mean LS values increased during liver fibrosis progression. There were significant differences in LS values between (F0 and F1) and (F2 and F3), (F2 and F3) and (F4), and (F0 and F1) and (F4), which are three clinically relevant fibrosis groups. There was a high correlation between the LS values measured by MRE and the stages of liver fibrosis determined by histology ($R^2 = 0.67$, $P < 0.001$). MRE imaging has the potential to serve as a noninvasive, unenhanced imaging technique for liver fibrosis diagnosis and staging.

Keywords: Liver fibrosis, magnetic resonance elastography, imaging biomarker, diagnosis

Introduction

Liver fibrosis is characterized by the progressive deposition of excess collagen, proteoglycans and other macromolecules in the extracellular matrix in response to repetitive liver injury caused by various chronic liver diseases [1-4]. The main causes of liver fibrosis include chronic viral hepatitis type B, chronic viral hepatitis type C, and alcohol abuse [1, 2]. Advanced liver fibrosis can lead to cirrhosis, liver failure, portal hypertension, and liver cancer, and often requires liver transplantation as a life-saving procedure. Therefore, the accurate staging of liver fibrosis and the diagnosis of early cirrhosis are critical for determining treatment strategies, assessing the therapeutic response, and stratifying the long-term prognosis [3].

When liver biopsy remains the gold standard for the diagnosis and staging of liver fibrosis, it has several limitations, such as sample error, inter-/intra-observer variability, risk, high cost, invasiveness, and complications [5-8]. It is necessary to develop noninvasive imaging approaches for the diagnosis staging and the dynamic evaluation of the effectiveness of liver fibrosis therapy.

Noninvasive imaging techniques, including ultrasound [9-11], computed tomography (CT) [11], blood oxygen level-dependent magnetic resonance imaging (BOLD-MRI) [12], diffusion-weighted MRI (DW-MRI) [13], and dynamic contrast material-enhanced MRI (DCE-MRI) [14], have been proposed for the diagnosis staging of liver fibrosis [15-19]. However, the ability to

detect early and intermediate stages of fibrosis with these techniques remains is limited [20-22]. A conventional ultrasound assessment of the hepatic vasculature is insufficient for detecting early and intermediate stages of fibrosis [9-11]. CT provides improved resolution of early morphological changes caused by cirrhosis but remains unhelpful for fibrosis detection [11]. Specific features of MRI, including functional techniques such as BOLD-MRI, DW-MRI, and DCE-MRI, reliably identify cirrhosis but remain unhelpful in detecting earlier stages of fibrosis [13, 14, 22].

Magnetic resonance elastography (MRE) is a very promising MR technique and has been considered a tool for quantifying the mechanical properties of tissue fibrosis [23, 24]. MRE has the potential as a noninvasive, unenhanced method for characterizing the progression of liver fibrosis, including the staging of liver fibrosis in various chronic liver diseases [25]. However, no studies have investigated the relationship between 3-T MRE measurements and dynamic progression of liver fibrosis in rabbit animal models. Therefore, the purpose of our study was to evaluate the 3-T MRE measurements of dynamic fibrosis progression by comparing to histologic studies in a rabbit model of liver fibrosis.

Materials and methods

All experiments in this study were approved by the institutional animal care committee and were performed in accordance with institutional guidelines.

Animal model and experimental design

Sixty New Zealand male rabbits between 3 and 4 months of age that initially weighed 1.6 to 2.1 kg were used for the experiments. The rabbits were randomly divided into two groups: a liver fibrosis group (n = 44) and a control group (n = 16).

Each rabbit in the liver fibrosis group received weekly subcutaneous injections in the neck and back comprising 50% carbon tetrachloride (CCl_4) in oily solution (0.1 ml/kg at 1-3 weeks, 0.2 ml/kg at 4-6 weeks, 0.3 ml/kg at 7-9 weeks) [26, 27]. Control rabbits received subcutaneous injections with the same amount of normal saline solution instead.

MRI was performed on four control rabbits and CCl_4-injected rabbits at 4, 5, 6 and 10 weeks and on the remaining twelve CCl_4-injected rabbits at 10 weeks (each time point n = 8).

MRE measurements

After fasting overnight, the animals were anesthetized by an intramuscular injection of sierra oxazine hydrochloride (0.1 ml/kg), and fifteen minutes later, they were intravenously injected with 3% pentobarbital solution (0.1 ml/kg) in the ear margin vein. Rabbits were placed in the supine position and fixed with an abdominal elastic belt to secure the passive driver to the abdominal wall and restrain abdominal movement. All MRI acquisitions were performed using a 3-T MRI Scanner (Magnetom Spectra, Siemens Healthcare, Erlangen, Germany) with an 18-channel knee-joint coil (Siemens Healthcare).

Liver location turbo spin-echo (TSE) T1-weighted (T1W) and TSE T2-weighted (T2W) anatomical scans were performed to verify rabbit positioning and liver presence. The T1W scan parameters were a repetition time (TR)/echo time (TE) of 165/2.92 ms, a flip angle (FA) of 70°, a slice thickness of 5 mm, an interslice gap of 1 mm, a field of view (FOV) of 160 mm × 140 mm, and a matrix size of 256 × 168. The T2W scan parameters were a TR/TE of 4500/82 ms, an FA of 20°, a slice thickness of 5 mm, an interslice gap of 1 mm, an FOV of 160 mm × 120 mm, and a matrix size of 256 × 144. For liver MRE, a 10-cm-diameter acoustic driver was placed against the body wall over the liver with the animal in the supine position and held in place with an abdominal binder. Sinusoidal acoustic waves (60 Hz) were applied during imaging with a MRE phase contrast gradient echo sequence (steady-state free precession gradient-recalled echo sequence). The frequency of motion-encoding gradients was synchronized with the shear wave excitation. Wave data were acquired with four phase offsets, and a modified, direct-inversion algorithm with multiscale capability was used to estimate liver stiffness. The sequence parameters were a TR/TE of 50/22.7 ms, a slice thickness of 5 mm, an FOV of 160 mm ×

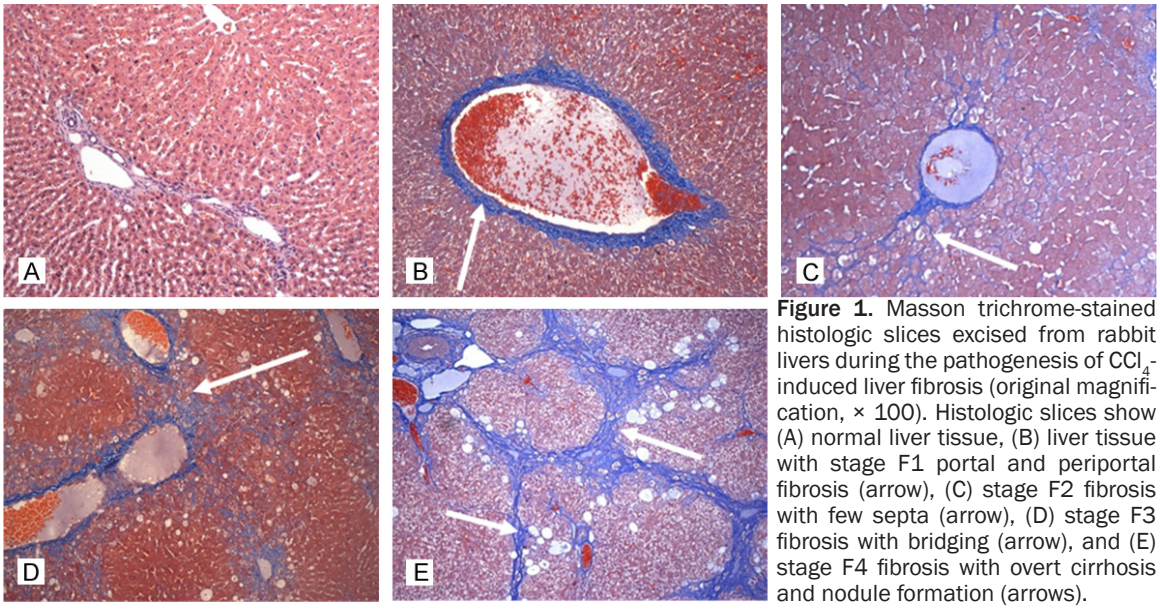

Figure 1. Masson trichrome-stained histologic slices excised from rabbit livers during the pathogenesis of CCl_4-induced liver fibrosis (original magnification, × 100). Histologic slices show (A) normal liver tissue, (B) liver tissue with stage F1 portal and periportal fibrosis (arrow), (C) stage F2 fibrosis with few septa (arrow), (D) stage F3 fibrosis with bridging (arrow), and (E) stage F4 fibrosis with overt cirrhosis and nodule formation (arrows).

Table 1. Liver stiffness assessment with MRE

	Sample size	Liver stiffness (kPa)	
		Value range	Mean ± SD
F0	15	0.75-1.36	1.06 ± 0.14
F1	11	1.09-1.73	1.30 ± 0.20
F2	8	1.12-1.66	1.40 ± 0.16
F3	7	1.46-2.26	1.85 ± 0.24
F4	12	2.13-4.36	2.86 ± 0.69
F-value (welch)			19.91
P-value			0.00

130 mm, and a matrix size of 96 × 96. The spatial resolution of the images was 0.5 × 0.5 × 0.5 mm. The number of wave phases was 4. A spatial pre-saturation pulse was applied to both sides of each slice selection to reduce blood flow motion artifacts. Three axial slices were acquired for each rabbit. Slices were acquired one at a time, and each slice took 22 s.

Image analysis

An inversion algorithm was applied to the wave phase images to generate quantitative images, called elastograms, which depict tissue stiffness. Regions of interest (ROIs) conforming to the liver margins but excluding major blood vessels were manually drawn on all three slices and averaged to produce a measure of shear stiffness. Five ROIs per slice were manually placed on the T1W image and elastogram simultaneously. The mean LS value for each rabbit was expressed in kilopascals (kPa) [28].

Histologic evaluation

After the MR examinations, each rabbit was immediately euthanized with in intravenous injection of a lethal amount (7-10 ml) of xylazine hydrochloride under deep anesthesia. Three histologic slices that were excised from the left lateral, right lateral, and medium lateral liver lobes of each rabbit were fixed in 10% buffered formaldehyde solution and embedded in paraffin for the histologic evaluation. Masson trichrome staining was used to identify collagen tissue. A pathologist (with > 10 years of experience) first assessed the stage of liver fibrosis semiquantitatively according to the Scheuer scoring system [29]. Stage F0 indicates no fibrosis, stage F1 indicates portal fibrosis without septa, stage F2 indicates portal fibrosis with few septa, stage F3 indicates numerous septa without cirrhosis, and stage F4 indicates cirrhosis. The Masson trichrome-stained slides were then digitized with optical magnification (× 100) using an imaging post-processing system (Image-Pro Express 5.1.1.14, Rockville, MD). Next, one of the authors of this study performed a quantitative analysis of liver fibrosis on an average of 30 fields per section. On the stained slides, collagen fibers were stained with aniline blue, and hepatocytes were stained red. The fibrotic region was identified by extracting the area of blue components with the use of offline

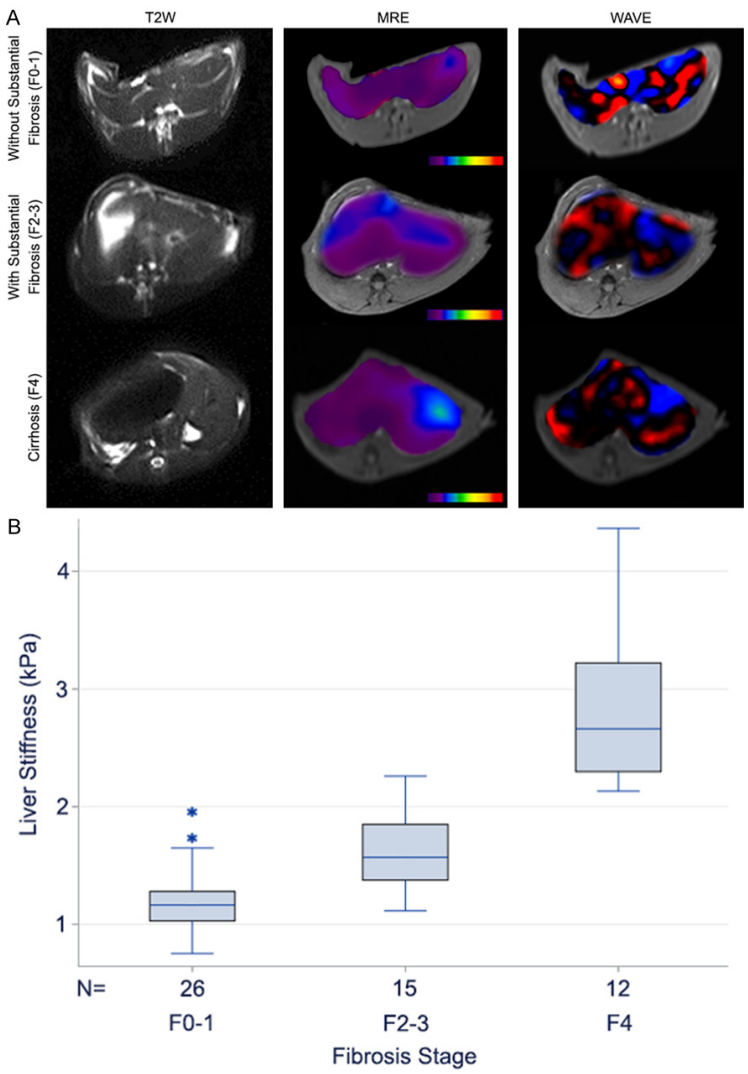

Figure 2. Increasing LS with increasing fibrosis stage. A: Transverse turbo spin-echo anatomic T2W MR images (left), corresponding MRE maps (middle) and wave images (right) show liver without substantial fibrosis (in control rabbit F0, LS = 1.06 kPa), liver with substantial (stage F2) fibrosis (LS = 1.85 kPa), and liver with cirrhosis (stage F4, LS = 3.11 kPa). B: Box plot shows mean hepatic LS values for rabbits in stage F0-F1, stage F2-F3, and stage F4 fibrosis groups. Bottom boundary of each box (closest to zero) indicates 25th percentile, horizontal line in each box indicates median value, and top boundary of each box (farthest from zero) indicates 75th percentile. Error bars indicate 10th and 90th percentiles. Outlier (*) is also shown.

Table 2. Liver stiffness values at different fibrosis stages

Liver Fibrosis Group	No. of Rabbits	Liver Stiffness Values (kPa)*
F0-1	26	1.19 ± 0.26†
F2-3	15	1.61 ± 0.30‡
F4	12	2.86 ± 0.69†,‡

*Data are means ± standard deviations. †$P < .05$ for comparison with rabbits in stage F2-3 group. ‡$P < .05$ for comparison with rabbits in stage F0-1 group.

ImageJ post-processing software (National Institutes of Health, Bethesda, MD). Fibrotic deposition was expressed as the ratio of stained collagen tissue area to the total area measured in the analyzed field.

Statistical analysis

LS values were compared at each pathological stages using Welch's ANOVA. MRE LS values were compared between the three groups (rabbits without substantial fibrosis, stages F0 and F1; rabbits with substantial fibrosis, stages F2 and F3; and rabbits with cirrhosis, stage F4) using ANOVA followed by two-by-two comparisons performed with independent-sample t-tests. The relationship between LS and pathological stage was assessed using Spearman correlation coefficients. To evaluate the ability of MRE to differentiate between stages, the rabbits were grouped into four categories based on pathological results [12]: stages ≥F1 (including F1+2+3+4), stages ≥F2 (F2+3+4), stages ≥F3 (F3+4), and stage 4. A receiver operating characteristic (ROC) curve was used to assess the performance of MRE over a range of sensitivity and specificity values. The area under the curve (AUC) was measured to obtain information for evaluating the ability for MRE to distinguish fibrotic liver stages. Statistical analysis results were considered to be significant at $P < 0.05$. All statistical analyses were performed using SPSS software (SPSS 19.0, Chicago, IL).

Results

Of the sixty rabbits, six in the liver fibrosis group died during the experiment. One rabbit in the control group was excluded due to stubborn snuffles. A total of fifty-three rabbits completed the study, with fifteen of those at stage F0 (control group). In the liver fibrosis group, eleven

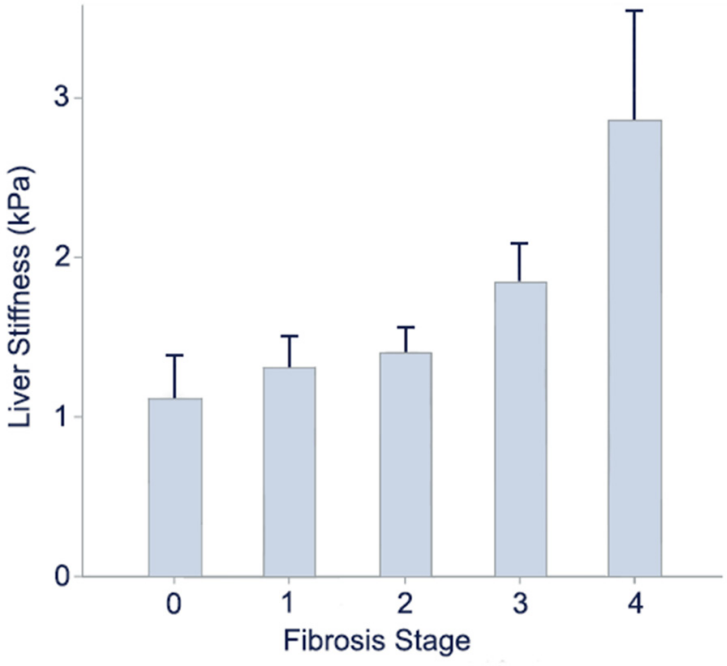

Figure 3. LS values in different stages. Graph shows that there are significant differences in LS values between F0 and F2, F0 and F3, F0 and F4, F1 and F3, and F1 and F4 (all $P < 0.05$); there are no significant differences in LS values between F0 and F1, F1 and F2, and F3 and F4 (all $P > 0.05$).

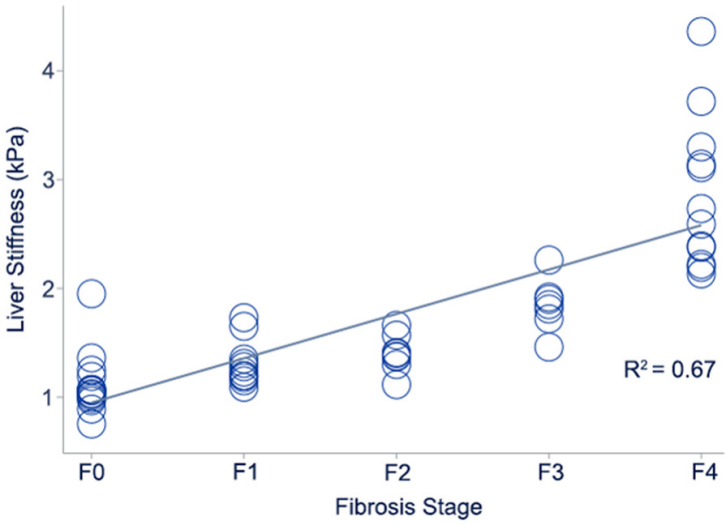

Figure 4. The relationship between the LS and liver fibrosis stages. Scatterplot shows that there is a significant correlation between LS values and liver fibrosis stages ($R2 = 0.67$, $P < 0.001$).

were obtained from stage F0, F2 and F4 rabbits (**Figure 2A**). Mean LS values were 1.19 ± 0.26 kPa for the rabbits without substantial fibrosis (stages F0 and F1), 1.61 ± 0.30 kPa for the rabbits with substantial fibrosis (stages F2 and F3), and 2.86 ± 0.69 kPa for the rabbits with cirrhosis (stage F4) (**Figure 2B** and **Table 2**). There were significant differences in the LS values between (F0 and F1) and (F2 and F3), (F2 and F3) and (F4), and (F0 and F1) and (F4). The mean LS values increased during liver fibrosis progression, from 1.06 ± 0.14 kPa in control rabbits (F0) to 1.30 ± 0.20 kPa (F1), 1.40 ± 0.16 kPa (F2), 1.85 ± 0.24 kPa (F3), and 2.86 ± 0.69 kPa (F4). There are significant differences in LS values between F0 and F2, F0 and F3, F0 and F4, F1 and F3, and F1 and F4 (all $P < 0.05$); there are no significant differences in LS values between F0 and F1, F1 and F2, and F3 and F4 (all $P > 0.05$). There are significant differences in the LS values between F0 and F2, F0 and F3, F0 and F4, F1 and F3, and F1 and F4 (all $P < 0.05$); there are no significant differences in the LS values between F0 and F1, F1 and F2, and F3 and F4 (all $P > 0.05$) (**Figure 3**). There were significant differences in the mean LS values between animals at stages F0 and F1 and those at stages F2 and F3 ($P = 0.006$), between animals at stages F2 and F3 and those at stage F4 ($P = 0.001$), and between animals at stages F0 and F1 and those at stage F4 ($P < 0.001$). There was a significant correlation between histological stages and LS values ($R^2 = 0.67$, $P < 0.01$) (**Figure 4**).

rabbits were stage F1, eight were stage F2, seven were stage F3, and twelve were stage F4 (**Figure 1**).

The MRE of LS values (mean ± SD) are shown in **Table 1**. The T2W, MRE and shear wave images

The diagnostic ability of MRE for liver fibrosis was calculated with a ROC analysis. The AUCs of the ROC curve for LS values at different stages of fibrosis were ≥F1, 0.96 ± 0.03; ≥F2, 0.95 ± 0.03; ≥F3, 0.992 ± 0.01; and F4, 0.99 ± 0.01 (**Figure 5**). The optimal threshold value, sensi-

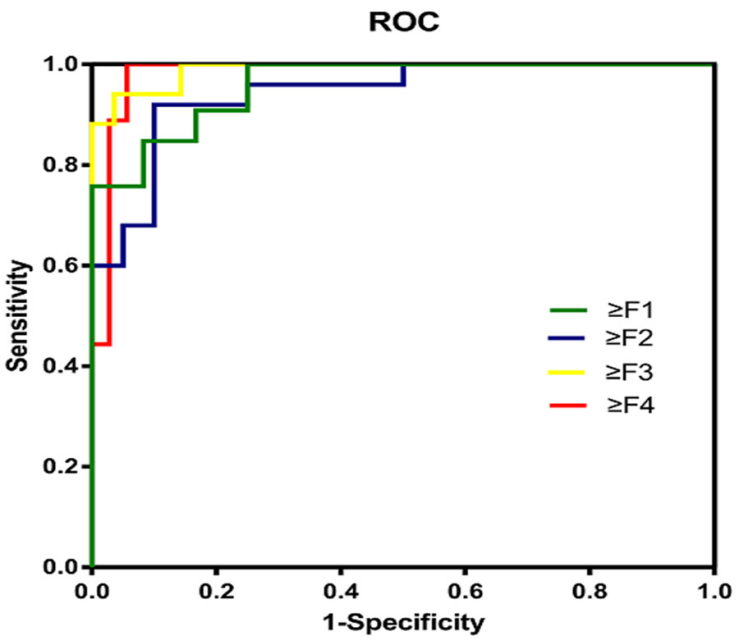

Figure 5. ROC analysis of the diagnostic ability of MRE for hepatic fibrosis. Four ROC curves are shown to indicate the ability of this MRE protocol to discriminate each fibrosis stage. The green curve shows F0 vs. F1-4, and the AUC of the ROC curve was 0.96, with a cut-off value of 1.105 kPa. Sensitivity, specificity and accuracy were 97.4%, 80.0% and 92.5%, respectively. The blue curve shows F0-1 vs. F2-4, and the AUC of the ROC curve was 0.954, with a cut-off value of 1.365 kPa. Sensitivity, specificity and accuracy were 92.6%, 92.3% and 92.5%, respectively. The yellow curve shows F0-2 vs. F3-4, and the AUC of the ROC curve was 0.992, with a cut-off value of 1.69 kPa. Sensitivity, specificity and accuracy were 94.7%, 97.1% and 96.2%, respectively. The red curve shows F0-3 vs. F4, and the AUC of the ROC curve was 0.99, with a cut-off value of 2.027 kPa. Sensitivity, specificity and accuracy were 100%, 97.6% and 98.1%, respectively.

Table 3. Diagnostic test characteristics of LS values from 2D-MRE in detection of liver fibrosis staging

	≥F1	≥F2	≥F3	F4
Cut-off (kPa)	1.11	1.37	1.69	2.03
AUC	0.96 ± 0.03	0.95 ± 0.02	0.99 ± 0.01	0.994 ± 0.01
Sensitivity (%)	97.4	92.6	94.7	100
Specificity (%)	80.0	92.3	97.1	97.6
Accuracy (%)	92.5	92.5	96.2	98.1
PPV (%)	92.5	92.6	94.7	92.3
NPV (%)	92.3	92.3	97.1	88.9
F-value	42.59	29.63	19.79	12.473
P-value	< 0.0001	< 0.0001	< 0.0001	< 0.0001

LS, liver stiffness; AUC, areas under the ROC curve; PPV, Positive predictive value; NPV, Negative predictive value.

tivity, specificity, accuracy rating, positive predictive value, and negative predictive value of the LS values for different groups are shown in **Table 3**.

Discussion

Liver fibrosis and cirrhosis develop gradually, and patients are initially asymptomatic [30]. As demonstrated over the past 10 years, even advanced fibrosis can be reversed with proper detection and treatment [30, 31]. Early diagnosis is essential if medications that can potentially mitigate the progression of the disease are to be used.

Laboratory tests, such as serum liver enzyme levels and fibrosis score panels, are neither accurate for distinguishing intermediate stages of liver fibrosis nor specific for liver fibrosis [32]. By using noninvasive diagnosis and staging methods, we could avoid the complications and sampling errors that are common with biopsy procedures while facilitating close, longitudinal follow-up of the treatment response. BOLD-MRI and DCE-MRI have been proposed for the noninvasive diagnosis of liver fibrosis, and have demonstrated reliable identification of cirrhosis, but remain unhelpful with earlier stages of fibrosis [13, 14, 22].

With MRE, propagating mechanical shear waves travel faster in stiffer tissues and more slowly in softer tissues [23]. The wavelengths of the shear waves are longer in stiffer tissue and shorter in softer tissues. The shear waves are captured in a wave image, and an inversion algorithm processes the information to provide a measure of tissue stiffness [23, 33]. MRE uses dynamic low-frequency shear waves in the range of 20 to 200 Hz because their wavelengths in tissue are in the measurable range of millimeters, to tens of millimeters, and they undergo less attenuation compared with high-frequency waves. The principle aim of our study was to

detect the progression of liver fibrosis. In a rabbit model of CCl_4-induced liver fibrosis, we observed a significant correlation between MRE LS measurements and the progression of liver fibrosis. In addition, there was a significant correlation between LS and the severity of fibrosis.

In this study, CCl_4-induced diffuse liver fibrosis revealed cellular alterations and histologic patterns that were similar to those in human liver fibrosis [34]. In particular, this rabbit model shows the progressive stages of liver fibrosis from F0 to F4. However, the speed of fibrosis progression varies among animals. Therefore, a variable number of rabbits were at each stage of liver fibrosis in our study. Because of the relatively small sample, we not only compared the results of the Scheuer scoring system among the five stages but also observed significant differences in the LS responses among animals in each of the three clinically relevant fibrosis groups (no substantial fibrosis [stages F0 and F1], substantial fibrosis [stages F2 and F3], and cirrhosis [stage F4]) [35].

As liver fibrosis progressed, we observed significant increases in MRE LS measurements, histologic stages, and the MRE LS response to disease progression. This altered response may result from the presence of regenerative nodules and the fibrous bands or septa between them, which can cause distortion, compression, and even obliteration of the hepatic vasculature [36], or from the increased resistance of the portal venous blood flow and the formation of intrahepatic portosystemic functional shunts [37].

This study showed that MRE LS is an effective imaging biomarker for differentiating normal and fibrotic livers and has a very high negative predictive value of 92.3%.

A linear relationship between the LS measurement and the stage of hepatic fibrosis fits well in this animal model. The ROC analysis showed cut-off stiffness values of 1.105 kPa (≥F1), 1.365 kPa (≥F2), 1.690 kPa (≥F3), and 2.027 kPa (F4). The sensitivity and specificity of MRE were 90.4% and 80% in stage ≥F1, 92.6% and 92.3% in stage ≥F2, 94.7% and 97.1% in stage ≥F3, and 100% and 97.6% in stage F4, respectively. Therefore, MRE could also be helpful for screening in anti-fibrotic clinical trials.

Compared with transient ultrasonic elastography (TUE), which is a clinically standard method [38, 39], MRE has several advantages. The stiffness of the whole liver can be observed and evaluated, and MRE can provide three-dimensional tissue elastic modulus values of ROIs, which do not need acoustic windows and are operator independent. TUE obtains one-dimensional tissue elastic modulus values that significantly restrict its application in patients with ascites or those who are obese due to the influence of fluid interference wave propagation and the limited depth of penetration [38, 39]. By contrast, MRE is less disturbed by fluid and can reach a depth of 10 cm, which is suitable for patients with ascites or obesity. A study reported that the success rate of MRE is 94%, which is much higher than that of TUE (84%). Nevertheless, MRE should be further studied, particularly for the early detection of hepatic fibrosis and the response to treatment [23, 40].

There were several limitations to the current study. First, the sample size was relatively small, although sixty rabbits were included. To our knowledge, this is largest rabbit sample for an MRE study of liver fibrosis. We measured the mean LS for the entire liver rather than for specific liver regions on each image section. It was difficult to co-register the MR images with the histologic specimens; however, CCl_4-induced fibrosis progresses homogeneously [41]. Second, we did not serially follow-up each animal and its fibrosis progression during the CCl_4-injection. Rather, we performed MRI in each animal at a single time point because of the logistic complexities involved in serially following-up the animals during these processes and our desire for reference-standard histologic confirmation of the fibrosis stages, which required that we sacrifice each animal to harvest its liver. In future MRE studies, fibrosis progression could be followed in each animal. Finally, MRE on humans is usually performed in a breath-holding state, but respiratory motion artifacts could not be fully avoided with experimental animals.

MRE is a promising method for the noninvasive diagnosis and staging of liver fibrosis. In a rabbit model of CCl_4-induced fibrosis, we observed a significant correlation between the LS response and the degree of liver fibrosis. In particular, our results show that the MRE approach

is feasible for longitudinal research of fibrosis progression from the early stages of liver fibrosis to liver cirrhosis, and this research can be translated for the dynamic evaluation of the effectiveness of liver fibrosis therapy.

Acknowledgements

This study was supported by grants from Shenzhen Municipal Committee of Science and technology innovation (No. JCYJ20150403091-443308), Health and Family Planning Commission of Shenzhen Municipality (No. 2015010-43) and U.S.A. National Cancer Institute (R01-CA196967).

Disclosure of conflict of interest

None.

Authors' contribution

X.W. and Z.Z. conceived and designed the study. L.Z., J.J., B.S., C.W., W.L., and J.C. contributed experimental works. L.Z., J.J., B.S., C.W., and J.C. contributed collection, analysis of data and manuscript preparation. X.W., Z.Z. wrote and revised the manuscript.

Address correspondence to: Xing Wei, Department of Radiology, Affiliated Third Hospital of Suzhou University, Juqian Street 185, Tianning District, Changzhou 213000, Jiangsu Province, China. Tel: +86-0519-68870065; Fax: +86-0519-68870065; E-mail: suzhxingwei@sina.cn; Zhuoli Zhang, Department of Radiology, Feinberg School of Medicine, Northwestern University, Robert H. Lurie Comprehensive Cancer Center 737 N. Michigan Ave, 16th Floor, Chicago, IL 60611, USA. Tel: 312-926-3874; Fax: 312-926-5991; E-mail: zhuoli-zhang@northwestern.edu

References

[1] Venkatesh SK, Yin M, Takahashi N, Glockner JF, Talwalkar JA and Ehman RL. Non-invasive detection of liver fibrosis: MR imaging features vs. MR elastography. Abdom Imaging 2015; 40: 766-775.

[2] Venkatesh SK, Xu S, Tai D, Yu H and Wee A. Correlation of MR elastography with morphometric quantification of liver fibrosis (Fibro-C-Index) in chronic hepatitis B. Magn Reson Med 2014; 72: 1123-1129.

[3] Batheja M, Vargas H, Silva AM, Walker F, Chang YH, De Petris G and Silva AC. Magnetic resonance elastography (MRE) in assessing hepatic fibrosis: performance in a cohort of patients with histological data. Abdom Imaging 2015; 40: 760-765.

[4] Loomba R, Wolfson T, Ang B, Hooker J, Behling C, Peterson M, Valasek M, Lin G, Brenner D, Gamst A, Ehman R and Sirlin C. Magnetic resonance elastography predicts advanced fibrosis in patients with nonalcoholic fatty liver disease: a prospective study. Hepatology 2014; 60: 1920-1928.

[5] Bravo AA, Sheth SG and Chopra S. Liver biopsy. N Engl J Med 2001; 344: 495-500.

[6] Standish RA, Cholongitas E, Dhillon A, Burroughs AK and Dhillon AP. An appraisal of the histopathological assessment of liver fibrosis. Gut 2006; 55: 569-578.

[7] Bedossa P, Dargere D and Paradis V. Sampling variability of liver fibrosis in chronic hepatitis C. Hepatology 2003; 38: 1449-1457.

[8] Talwalkar JA, Yin M, Fidler JL, Sanderson SO, Kamath PS and Ehman RL. Magnetic resonance imaging of hepatic fibrosis: emerging clinical applications. Hepatology 2008; 47: 332-342.

[9] Seo YS, Kim MN, Kim SU, Kim SG, Um SH, Han KH and Kim YS. Risk Assessment of Hepatocellular Carcinoma Using Transient Elastography Vs. Liver Biopsy in Chronic Hepatitis B Patients Receiving Antiviral Therapy. Medicine (Baltimore) 2016; 95: e2985.

[10] Bouzitoune R, Meziri M, Machado CB, Padilla F and Pereira WC. Can early hepatic fibrosis stages be discriminated by combining ultrasonic parameters? Ultrasonics 2016; 68: 120-126.

[11] Andersen SB, Ewertsen C, Carlsen JF, Henriksen BM and Nielsen MB. Ultrasound Elastography is Useful for Evaluation of Liver Fibrosis in Children-A Systematic Review. J Pediatr Gastroenterol Nutr 2016; 63: 389-99.

[12] Jin N, Deng J, Chadashvili T, Zhang Y, Guo Y, Zhang Z, Yang GY, Omary RA and Larson AC. Carbogen gas-challenge BOLD MR imaging in a rat model of diethylnitrosamine-induced liver fibrosis. Radiology 2010; 254: 129-137.

[13] Dyvorne HA, Jajamovich GH, Bane O, Fiel MI, Chou H, Schiano TD, Dieterich D, Babb JS, Friedman SL and Taouli B. Prospective comparison of magnetic resonance imaging to transient elastography and serum markers for liver fibrosis detection. Liver Int 2016; 36: 659-66.

[14] Noren B, Dahlstrom N, Forsgren MF, Dahlqvist Leinhard O, Kechagias S, Almer S, Wirell S, Smedby O and Lundberg P. Visual assessment of biliary excretion of Gd-EOB-DTPA in patients with suspected diffuse liver disease-A biopsy-verified prospective study. Eur J Radiol Open 2015; 2: 19-25.

[15] Afdhal NH and Nunes D. Evaluation of liver fibrosis: a concise review. Am J Gastroenterol 2004; 99: 1160-1174.
[16] Taouli B, Ehman RL and Reeder SB. Advanced MRI methods for assessment of chronic liver disease. AJR Am J Roentgenol 2009; 193: 14-27.
[17] Lee Y, Lee JM, Lee JE, Lee KB, Lee ES, Yoon JH, Yu MH, Baek JH, Shin CI, Han JK and Choi BI. MR elastography for noninvasive assessment of hepatic fibrosis: reproducibility of the examination and reproducibility and repeatability of the liver stiffness value measurement. J Magn Reson Imaging 2014; 39: 326-331.
[18] Yin M, Talwalkar JA, Glaser KJ, Manduca A, Grimm RC, Rossman PJ, Fidler JL and Ehman RL. Assessment of hepatic fibrosis with magnetic resonance elastography. Clin Gastroenterol Hepatol 2007; 5: 1207-1213, e1202.
[19] Faria SC, Ganesan K, Mwangi I, Shiehmorteza M, Viamonte B, Mazhar S, Peterson M, Kono Y, Santillan C, Casola G and Sirlin CB. MR imaging of liver fibrosis: current state of the art. Radiographics 2009; 29: 1615-1635.
[20] Yu X, Wu Y, Liu H, Gao L, Sun X, Zhang C, Shi J, Zhao H, Jia B, Liu Z and Wang F. Small-Animal SPECT/CT of the Progression and Recovery of Rat Liver Fibrosis by Using an Integrin alphabeta-targeting Radiotracer. Radiology 2016; 279: 502-12.
[21] Lombardi R, Buzzetti E, Roccarina D and Tsochatzis EA. Non-invasive assessment of liver fibrosis in patients with alcoholic liver disease. World J Gastroenterol 2015; 21: 11044-11052.
[22] Singal AG, Pillai A and Tiro J. Early detection, curative treatment, and survival rates for hepatocellular carcinoma surveillance in patients with cirrhosis: a meta-analysis. PLoS Med 2014; 11: e1001624.
[23] Mariappan YK, Glaser KJ and Ehman RL. Magnetic resonance elastography: a review. Clin Anat 2010; 23: 497-511.
[24] Singh S, Venkatesh SK, Loomba R, Wang Z, Sirlin C, Chen J, Yin M, Miller FH, Low RN, Hassanein T, Godfrey EM, Asbach P, Murad MH, Lomas DJ, Talwalkar JA and Ehman RL. Magnetic resonance elastography for staging liver fibrosis in non-alcoholic fatty liver disease: a diagnostic accuracy systematic review and individual participant data pooled analysis. Eur Radiol 2016; 26: 1431-40.
[25] Stasi C and Milani S. Non-invasive assessment of liver fibrosis: Between prediction/prevention of outcomes and cost-effectiveness. World J Gastroenterol 2016; 22: 1711-1720.
[26] Goncalves RV, Novaes RD, Sarandy MM, Leite JP, Vilela EF, Cupertino MD and da Matta SL. Schizocalyx cuspidatus (A. St.-Hil.) Kainul. & B. Bremer extract improves antioxidant defenses and accelerates the regression of hepatic fibrosis after exposure to carbon tetrachloride in rats. Nat Prod Res 2016; 1-5.
[27] Brandao CG, Ferreira HH, Piovesana H, Polimeno NC, Ferraz JG, de Nucci G and Pedrazzoli J Jr. Development of an experimental model of liver cirrhosis in rabbits. Clin Exp Pharmacol Physiol 2000; 27: 987-990.
[28] Loomba R, Cui J, Wolfson T, Haufe W, Hooker J, Szeverenyi N, Ang B, Bhatt A, Wang K, Aryafar H, Behling C, Valasek MA, Lin GY, Gamst A, Brenner DA, Yin M, Glaser KJ, Ehman RL and Sirlin CB. Novel 3D Magnetic Resonance Elastography for the Noninvasive Diagnosis of Advanced Fibrosis in NAFLD: A Prospective Study. Am J Gastroenterol 2016; 111: 986-94.
[29] Scheuer PJ and Maggi G. Hepatic fibrosis and collapse: histological distinction by orecin staining. Histopathology 1980; 4: 487-490.
[30] Shiratori Y, Imazeki F, Moriyama M, Yano M, Arakawa Y, Yokosuka O, Kuroki T, Nishiguchi S, Sata M, Yamada G, Fujiyama S, Yoshida H and Omata M. Histologic improvement of fibrosis in patients with hepatitis C who have sustained response to interferon therapy. Ann Intern Med 2000; 132: 517-524.
[31] Efremidis SC and Hytiroglou P. The multistep process of hepatocarcinogenesis in cirrhosis with imaging correlation. Eur Radiol 2002; 12: 753-764.
[32] Arora A and Sharma P. Non-invasive Diagnosis of Fibrosis in Non-alcoholic Fatty Liver Disease. J Clin Exp Hepatol 2012; 2: 145-155.
[33] Wagner M, Besa C, Bou Ayache J, Yasar TK, Bane O, Fung M, Ehman RL and Taouli B. Magnetic Resonance Elastography of the Liver: Qualitative and Quantitative Comparison of Gradient Echo and Spin Echo Echoplanar Imaging Sequences. Invest Radiol 2016; 51: 575-81.
[34] Yin M, Woollard J, Wang X, Torres VE, Harris PC, Ward CJ, Glaser KJ, Manduca A and Ehman RL. Quantitative assessment of hepatic fibrosis in an animal model with magnetic resonance elastography. Magn Reson Med 2007; 58: 346-353.
[35] Huwart L, Peeters F, Sinkus R, Annet L, Salameh N, ter Beek LC, Horsmans Y and Van Beers BE. Liver fibrosis: non-invasive assessment with MR elastography. NMR Biomed 2006; 19: 173-179.
[36] Blendis L and Wong F. The hyperdynamic circulation in cirrhosis: an overview. Pharmacol Ther 2001; 89: 221-231.
[37] Zoli M, Magalotti D, Bianchi G, Ghigi G, Orlandini C, Grimaldi M, Marchesini G and Pisi E. Functional hepatic flow and Doppler-assessed total hepatic flow in control subjects and in pa-

tients with cirrhosis. J Hepatol 1995; 23: 129-134.
[38] Pawlus A, Sokolowska-Dabek D, Szymanska K, Inglot MS and Zaleska-Dorobisz U. Ultrasound Elastography--Review of Techniques and Its Clinical Applications in Pediatrics--Part 1. Adv Clin Exp Med 2015; 24: 537-543.
[39] Barr RG, Ferraioli G, Palmeri ML, Goodman ZD, Garcia-Tsao G, Rubin J, Garra B, Myers RP, Wilson SR, Rubens D and Levine D. Elastography Assessment of Liver Fibrosis: Society of Radiologists in Ultrasound Consensus Conference Statement. Radiology 2015; 276: 845-861.
[40] Huwart L and van Beers BE. MR elastography. Gastroenterol Clin Biol 2008; 32: 68-72.
[41] Li Z, Sun J, Chen L, Huang N, Hu P, Hu X, Han G, Zhou Y, Bai W, Niu T and Yang X. Assessment of liver fibrosis using pharmacokinetic parameters of dynamic contrast-enhanced magnetic resonance imaging. J Magn Reson Imaging 2016; 44: 98-104.